

# The value of satellite retrieved snow cover images to assess water resources and the theoretical hydropower potential in ungauged mountain catchments

David Finger

*School of Science and Engineering, Reykjavík University, Reykjavík, Iceland; fingerd@gmx.net*

**Abstract** — *The estimation of water resources in ungauged areas is of major importance to develop adequate and sustainable water management strategies. Hydrological modelling can provide a powerful tool to assimilate hydro-meteorological data and estimate the total amount of water available from ungauged areas. Satellite images provide important information on the snow cover area in inaccessible mountain areas. The Hydrologiska Byråns Vattenbalansavdelning model (HBV) was used to estimate the total amount of snow, ice and rainfall runoff in two ungauged areas in north-eastern Iceland (Leirdalshraun, a 274 km<sup>2</sup> area above 595 m a.s.l. and Heljardalsfjöll, a 946 km<sup>2</sup> area above 235 m a.s.l.) that could potentially be used for hydropower production. The model parameters were determined using a multiple dataset calibration (MDC) relying on one year of satellite derived snow cover images and discharge data of gauged sub-catchments. Runoff from the ungauged area potentially used for hydropower exploitation was estimated using the parameter sets of the gauged sub-catchments. Snow cover in the ungauged areas as well as discharge in the gauged sub-catchments were validated over a 10 year validation period, revealing a robust simulation of snow melt in the entire area. The total amount of snow-melt, ice-melt and rainfall runoff available in Leirdalshraun and Heljardalsfjöll amounts up to ~690 M m<sup>3</sup> a<sup>-1</sup> and ~1190 M m<sup>3</sup> a<sup>-1</sup>, respectively. The theoretical potential energy of these water resources would account for up to 1.9 TWh a<sup>-1</sup>, a tremendous hydropower potential if the water could be collected in respective reservoirs and be deviated to turbines at sea-level. While the results are only valid for the specific case study, the modelling approach can be applied to any remote mountain area dominated by snow melt runoff.*

**Keywords:** Hydropower, model calibration, runoff, alpine hydrology, ungauged catchments, water resources.

## INTRODUCTION

Large scale hydrological modelling that includes areas with limited data availability has been identified as one of the key challenges facing hydrological research in the coming decade (McMillan *et al.*, 2016). Indeed, large scale modelling could provide valuable information about vital water resources for a wide variety of stake holders (Gupta *et al.*, 2014), ranging from drinking water supply to hydropower production to name just a few. Realistic modelling tools can help optimize water resources management of large watersheds (Wu *et al.*, 2015). Such evidence-based information could help develop resilience-based policies,

leading to a sustainable usage of this vital resource (Rockstrom *et al.*, 2014; Xu *et al.*, 2015). In the scope of global climate change, research on water resources and associated hydropower production in remote areas with limited data availability is of eminent importance to anticipate upcoming challenges.

One way of assessing runoff from ungauged catchments is by regionalizing model parameters and applying parameters sets from gauged catchments to catchments with similar characteristics (Merz and Blöschl, 2004; Sefton and Howarth, 1998; Seibert, 1999). This is a valuable method as long as representative catchment characteristics can be identified

and regionalized (Xu and Singh, 2004). Regionalization can become particularly difficult in the case of heterogeneous and porous underground such as karst systems in the Alps (Finger *et al.*, 2013; Jeannin *et al.*, 2013), complex topography with heterogeneous vegetation (El Maayar and Chen, 2006), glacier- and snowmelt-fed catchments (Hock, 2005) and catchments characterized by porous volcanics as in Iceland.

In recent years remotely sensed observations coupled to hydrological models have proven to enhance the estimation of water resources in ungauged basins. For example, Sun *et al.* (2010) demonstrated that remotely sensed river cross sections correlate well with discharge observations and Khan *et al.* (2011) used remotely mapped flood areas to improve predictions of ungauged watersheds. Brakenridge *et al.* (2012) used satellite retrieved discharge measurements to calibrate a global hydrology model. More recent studies concluded that remote sensing data can indeed reduce uncertainty when modelling large scale hydrological runoff (Lamouroux *et al.*, 2014; Pechlivanidis and Arheimer, 2015). In mountain areas where snow melt provides a major contribution to the runoff, satellite retrieved snow cover images have proven to improve hydrological modelling results (Duethmann *et al.*, 2014; Finger *et al.*, 2011; Koboltschnig *et al.*, 2008). Finally, remotely sensed snow water equivalent estimations (SWE) of snow depth are promising but have proven to have a high uncertainty (Dong *et al.*, 2005). While it would certainly be helpful to model SWE, for most modeling approaches the thickness of snow is irrelevant for instant snow melt computation, as degree day factors or the enhanced temperature index are independent of snow depth (Finger *et al.*, 2011; Jost *et al.*, 2012; Seibert and Vis, 2012).

A particularly challenging location to test new methods for estimating water resources in ungauged rivers is Iceland. Iceland's numerous glaciers cover over 10% of the island's surface and contain about 3600 km<sup>3</sup> of ice (Björnsson *et al.*, 2013). The biggest glacier, Vatnajökull (Figure 1), has an area of 8100 km<sup>2</sup> and rises up to 2110 m a.s.l.. Topography east of Vatnajökull is characterized by steep valleys that drain ice melt, snow melt and rain runoff into the surrounding regions, including the Neovol-

canic Zone. Mean annual precipitation in southeast Iceland can exceed 8000 mm a<sup>-1</sup> (Crochet *et al.*, 2007), which is more than 10 times the world average (Adler *et al.*, 2003; Xie and Arkin, 1997). High precipitation rates combined with glacier ice and snow melt lead to an annual runoff of over 10000 mm a<sup>-1</sup> in some regions (Jonsdottir, 2008). These conditions make Iceland ideal for low carbon emission and renewable hydropower production. In 2013, hydropower made up approximately 20% of renewable energy production, representing approximately 75% of the total electricity production in Iceland (Orkustofnun, 2014). In 2008, total electricity production from hydropower was approximately 12.5 TWh a<sup>-1</sup>, while the total technical potential for hydropower exploitation in Iceland has been estimated to account for up to 33 TWh a<sup>-1</sup> (Tómasson, 1981), with at least 11 TWh a<sup>-1</sup> unsuitable for exploitation based on flora and fauna protection, land conservation and ecological concerns (Steingrímsson *et al.*, 2007). Accordingly, hydropower is one of the main emphases of the Icelandic Master Plan for energy development (Steingrímsson *et al.*, 2007). In this regard, numerical modelling can provide a valuable tool in quantifying water availability and identifying suitable locations for hydropower production, thus providing fundamental knowledge for decision makers. In particular, satellite based snow cover images are important for assessment of ungauged catchments (Hall *et al.*, 2002). Results of such numerical simulations can provide valuable estimations on water availability to help select appropriate new hydropower sites.

This study demonstrates the added value of multi dataset calibration (MDC) (Etter *et al.*, 2017; Finger *et al.*, 2011, 2015) to estimate snow, ice and rainfall runoff from two ungauged catchments in eastern Iceland (Leirdalshraun, a 274 km<sup>2</sup> area above 595 m a.s.l. and Heljardalsfjöll, a 946 km<sup>2</sup> area above 235 m a.s.l.). Both areas could potentially be used for hydropower production as they are characterized by high precipitation rates, snow- and glacier melt and steep slopes. To calibrate and validate the hydrological model, daily discharge data from nearby sub-catchments and daily satellite derived snow cover images of the entire area (Hall *et al.*, 2010; Hall *et al.*,

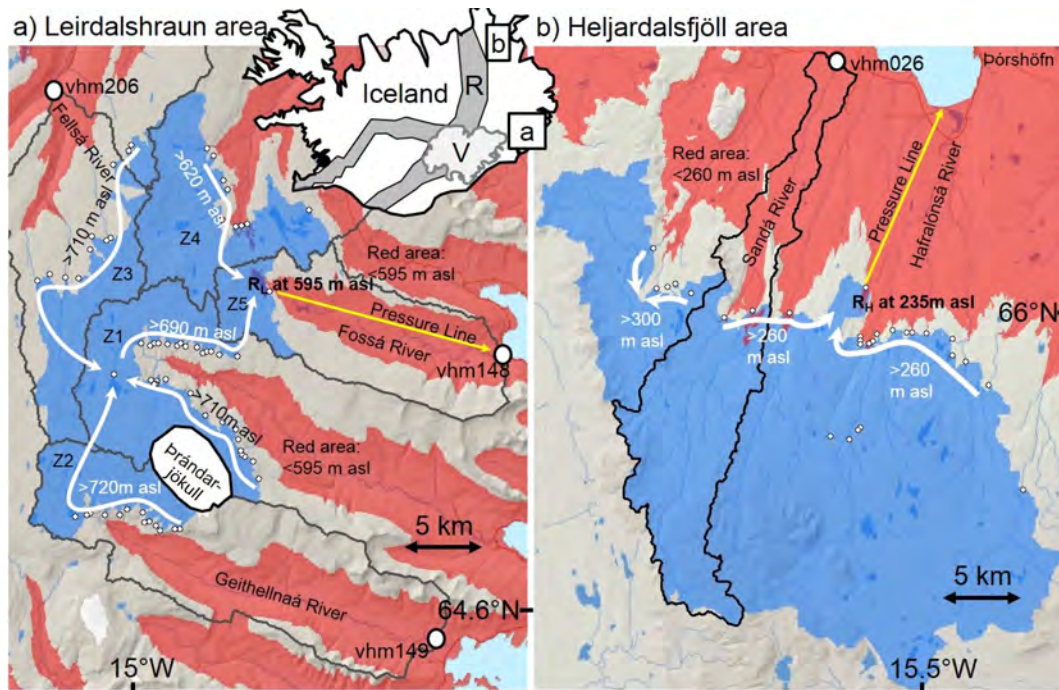


Figure 1. Overview of the Leirdalshraun and the Heljardalsfjöll areas located at a and b in the Iceland map, respectively. Dark grey area in the Iceland map illustrates the Neovolcanic Zone (labelled with R on the Iceland inset) is dark grey and Vatnajökull light grey (V). White dots represent potential water intakes where water will be collected and deviated into a potential water reservoir ( $R_L$  and  $R_H$ ). White arrows indicate flow direction in potential water pipelines. Yellow arrow indicates pressure pipes to a potential power station. Large white circles locate discharge gauging stations labelled with vhm and the respective serial number. Red area designates area lower than the reservoir for each study area. – *Yfirlitskort af Leirdalshrauni og Heljardalsfjöllum, staðsetning er merkt a og b á Íslandskortinu. Dökkgráa svæðið afmarkar gosbelti Íslands (R) og ljósgráa svæðið Vatnajökul (V). Hvítir punktar gefa til kynna möguleg vatnsinntök þar sem vatni verður safnað saman í hugsanleg vatnslón ( $R_L$  og  $R_H$ ). Hvítar örvar sýna flæðisstefnur pípuvatnslína. Gular örvar sýna þrýstipípur að mögulegri afstöð. Stóru hvítu hringirnir sýna staðsetningu mælistöðva merktum vhm og viðeigandi númerum. Rauð svæði gefa til kynna svæði sem liggja lægra en vatnslónin á hvoru rannsóknarsvæðanna.*

2002) were used. The study concludes by estimating the potential for hydropower production in the two ungauged areas. While the numeric results of this study are only valid for this specific case study, the modelling approach could be applied to large scale hydrological modelling anywhere in the world.

### STUDY SITES AND DATA

In the framework of the master plan for geothermal and hydropower development in Iceland (Steingrímsson *et al.*, 2007), the National Energy Authority of

Iceland (NEA, Orkustofnun) identified two study sites for potential new hydropower installations in eastern and north-eastern Iceland (Figure 1). The delineation of the area for hydropower exploitation defined by the NEA considered ecological concerns and the legal aspects provided by the Environmental Impact Assessment Act (No. 106, 25 May 2000). The first study site is located in the highlands, ~20 km northeast from Vatnajökull in an area hereafter called Leirdalshraun, comprising the glacier Þrándarjökull (Figure 1a). The

second study site is located about  $\sim 150$  km north of Vatnajökull, comprising the headwaters of the rivers Sandá and Hafalónsá (Figure 1b) hereafter called Heljardalsfjöll. The topography for both study sites was obtained from a digital elevation model with 25 m grid size provided by the Icelandic Geodetic Survey (Landmælingar). Three vegetation zones (grassland, swamps and areas without vegetation) were identified based on digital land cover maps from the CORINE programme of the European Environmental Agency (Moss and Wyatt, 1994).

A description of the two catchments is given in the following sections and the main characteristics and hydrometeorological data are summarized in Table 1 and Figure 2, respectively.

### The Leirdalshraun area

Leirdalshraun is located in eastern Iceland in the vicinity of Þrándarjökull (Figure 1a). The entire area is characterized by Tertiary basalt formation dating 3.3 to 16 million years ago. The NEA has classified the majority of this area as 'direct snow melt runoff' (Sigurdsson and Einarsson, 1988; Sigurdsson *et al.*, 2006) with little to no groundwater contribution. The potentially usable drainage area for hydropower exploitation extends over five sub-catchments, comprising a total area of 274 km<sup>2</sup> located above 595 m elevation. The highest elevation of the area is the top of Þrándarjökull, reaching an elevation of 1231 m a.s.l.. Water intakes in the five sub-catchments (Z1 to Z5 in

Figure 1a) would have to be connected with pipelines in order to collect and deviate water into a reservoir  $R_L$  at an elevation of 595 m a.s.l.. For this purpose, water intakes at numerous locations would have to be installed to collect the discharge in small mountain creeks and surface runoff from the designated hydropower exploitation area. The collected water would be stored in reservoir  $R_L$  and subsequently be used for power production by supplying it through pressure pipes to a power station at sea level close to the shore.

Daily discharge in the rivers Geithellnaá, Fossá and Fellsá are available from three gauging stations (vhm149 at an elevation of 17 m a.s.l., vhm148 at 26 m a.s.l. and vhm206 at 114 m a.s.l., respectively) operated by the Icelandic Meteorological Office (IMO). Discharge monitoring started in 1991 with a 7 year disruption from the end of 1998 to spring 2006. The gauging station of River Geithellnaá (sub-catchment Z2) is the only gauging station that drains a partially glacierized watershed. This watershed comprises parts of Þrándarjökull, which covers about 5.7% of the entire Leirdalshraun area. Most of the melt water from Þrándarjökull would also be collected in water intakes and deviated in pipelines into the reservoir  $R_L$  for storage. Accordingly, it is essential to account for glacier melt when modelling the Leirdalshraun area and therefore only discharge data from River Geithellnaá (station vhm149) can be used to calibrate ice melt parameters.

Table 1. Overview of catchment characteristics. – *Yfirlit mismunandi vatnsöfnunarsvæða.*

Name	Type <sup>(1)</sup>	Area km <sup>2</sup>	Elev. m a.s.l. min max		Glacier- ization mm a <sup>-1</sup>	Ann. <sup>(2)</sup> Precip. %	PET <sup>(3)</sup> mm a <sup>-1</sup>	Annual discharge m <sup>3</sup> s <sup>-1</sup> mm a <sup>-1</sup>		$P_{corr}$ <sup>(4)</sup>
Leirdalshraun east Iceland	D	274	595	1231	5.7	2441	$\sim 480$	Ungauged		
Geithellnaá vhm149	D	189	17	1231	3.5	2772	$\sim 480$	16.4	2734	0.99
Fossá vhm148	D	115	26	859	0	2541	$\sim 480$	8.3	2261	0.89
Fellsá vhm206	D	126	114	937	0	1777	$\sim 480$	7.3	1826	1.03
Heljardalsfjöll area	D	946	235	985	0	1441	$\sim 420$	Ungauged		
Sandá vhm026	G	266		980	0	1312	$\sim 420$	12.4	1589	1.3

(1) Characterization of the watershed according to Sigurdsson *et al.* (2006); D: primarily direct runoff; G: erosive soils, pot. groundwater contribution.

(2) Based on areal averages between 1991 and 2010, computed from gridded data as described in Crochet *et al.* (2011).

(3) Potential evapotranspiration (PET) as estimated by Einarsson (1972).

(4) The empirical  $P_{corr}$  factor is defined by the ratio of annual discharge and annual precipitation.

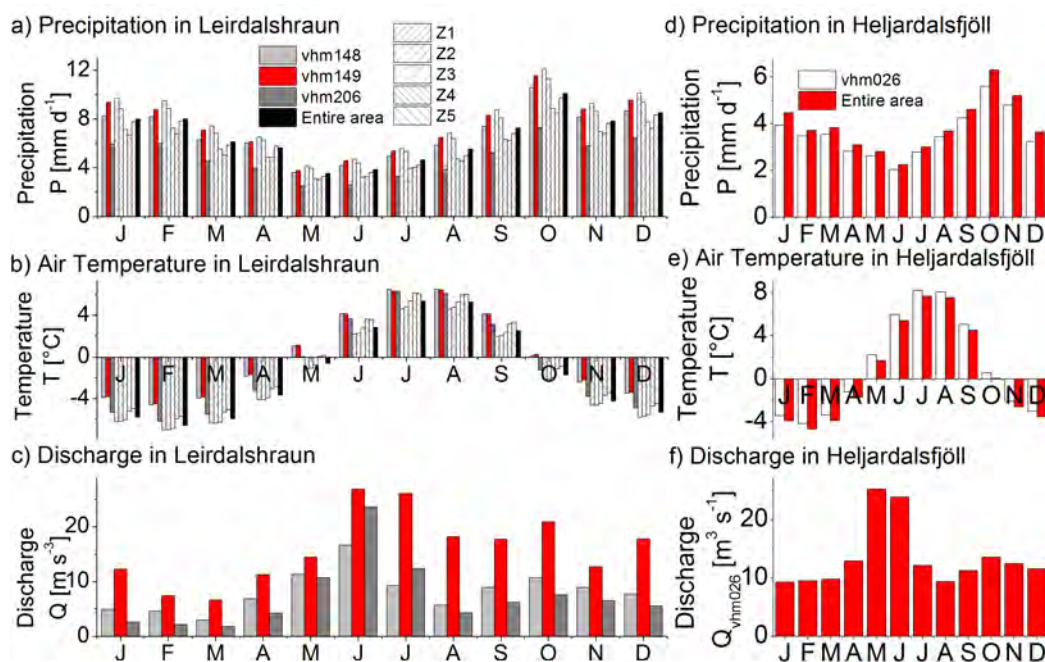


Figure 2. Average monthly hydro-meteorological observations from 1991 to 2010 in sub-catchments of Leirdalshraun and Heljardalsfjöll. a), b) and c) Observations of precipitation, temperature and discharge in Leirdalshraun, respectively and d), e) and f) for Heljardalsfjöll. – *Mánaðarmeðaltöl vatnafars- og veðurfræðithugana innan vatnasvæða Leirdalshrauns og Heljardalsfjalla, frá 1991 til 2010. a), b), c) Mælingar á úrkomu, hitastigi og leysingum í Leirdalshrauni og fyrir Heljardalsfjöll, d), e), f).*

Mean daily precipitation, air temperature and discharge rates for all available sub-catchments are illustrated in Figure 2a,b,c, respectively. Precipitation and temperature data were derived from the gridded data set described in Crochet *et al.* (2007) and Crochet and Johannesson (2011). Monthly mean precipitation reaches a maximum of over 10 mm d<sup>-1</sup> in October and a minimum of 5 mm d<sup>-1</sup> in May and June (Figure 2a). Mean monthly air temperatures drops to -5°C in winter and reaches about 5°C in summer (Figure 2b). The typical regional weather patterns of wet ocean air coming from the east can clearly be identified by the seasonal patterns of the five sub-catchments. The sub-catchments on the eastern slopes (Z1, Z2 and the watersheds of vhm149 and vhm148) receive about 30% more precipitation than the western slopes. In total, 2441 mm a<sup>-1</sup> (equivalent to 669 million m<sup>3</sup> a<sup>-1</sup>) precipitation falls on the

entire Leirdalshraun area. The annual discharge measured at the three gauging stations (vhm148, vhm149 and vhm206) compares adequately to the estimated mean areal precipitation in the corresponding watersheds (Figure 2c), revealing less than 10% discrepancy (Table 1). The discrepancy can be attributed to evapotranspiration (Einarsson, 1972), glacial mass change of Þrándarjökull, karstic flow pathways across topographic water divides and uncertainties in the discharge data (Coxon *et al.*, 2015).

### The Heljardalsfjöll area

The Heljardalsfjöll area is located in north-eastern Iceland in the headwaters of the rivers Sandá and Hafalónsá (Figure 1b). Almost the entire area is characterized by Plio-Pleistocene formations (aging between 0.7 and 3.3 million years) and Upper Pleistocene formations (aging less than 0.7 million years). While the headwaters of Heljardalsfjöll are character-

ized by direct snow melt runoff, the areas closer to the Neovolcanic Zone are permeable and it is assumed that water infiltrates and diffuses through the adjacent underground (Sigurdsson, 1990; Sigurdsson and Einarsson, 1988; Sigurdsson *et al.*, 2006). The Heljardalsfjöll area is over 150 km north of Vatnajökull and does not include any glacierized areas within its perimeter. The potential drainage area for hydropower production is visualized in Figure 1b and encloses a total area of 946 km<sup>2</sup>. The highest elevation of the area is close to the source of the River Sandá at 985 m a.s.l.. In order to collect all the water from the Heljardalsfjöll area, over 25 water intakes would have to be installed above the 260 m a.s.l. altitude line to collect and divert runoff into the reservoir R<sub>H</sub> at 235 m a.s.l.. The collected water could be stored in R<sub>H</sub> and delivered through pressure pipes to a power station at sea level close to the village of Þórshöfn.

Mean annual precipitation in the entire Heljardalsfjöll area amounts up to 1441 mm a<sup>-1</sup>, implying about 40% less precipitation than in the Leirdalshraun area (Table 1). Monthly precipitation (Figure 2d) reaches a maximum in October (~6 mm d<sup>-1</sup>) and a minimum in June (~3 mm d<sup>-1</sup>) while monthly air temperature rises during the summer month up to 8°C and drops below -4°C in winter (Figure 2e).

In the watershed of River Sandá, precipitation rates are about 9% lower than in the entire ungauged area, indicating that precipitation increases with altitude. At the gauging station vhm026, maximum monthly discharge rates of 25 m<sup>3</sup> s<sup>-1</sup> are recorded in May, when snow melt is expected to be most intense. Mean annual precipitation in the drainage area of vhm026 is estimated to amount up to 1312 mm a<sup>-1</sup>, which is about 20% less than observed runoff (1589 mm a<sup>-1</sup>) at the gauging station. Previous studies have observed similar discrepancies between precipitation and runoff, arguing that estimated precipitation has to be corrected by up to 20% to balance the water budget with the watershed (Einarsson and Jónsson, 2010; Gröndal, 2002; Þórarinsdóttir, 2012). However, the discrepancy within the water balance can also be explained by external water sources infiltrating from outside the topographic watershed of River Sandá. This hypothesis is fortified by the

monthly low flow discharge patterns during winter of more than 9 m<sup>3</sup> s<sup>-1</sup> (Figure 2f), even though air temperatures are below freezing and thus preventing any melt or surface runoff generation. Einarsson and Jónsson (2010) demonstrated that the discrepancies between precipitation and discharge is probably due to an external groundwater source. Such an external water contribution can be explained by the Neovolcanic Zone (Figure 1), (Einarsson, 2008; Gislason, 2008) potentially leading melt water from the western part of Vatnajökull to the watersheds of rivers Sandá and Hafralónsá (Egilson and Stefánsdóttir, 2014). Based on these more recent studies and the newer precipitation data sets (Crochet *et al.*, 2007), it must be assumed that an external groundwater contribution leads to the observed discrepancy in the watershed of River Sandá.

#### Remotely sensed snow cover data

Daily snow cover images with ~500 m spatial resolution for all watersheds were derived from the Moderate Resolution Imaging Spectroradiometer (binary MODIS product MOD10A1 V005), available online since 2000 (<http://nsidc.org/>) (Hall *et al.*, 2002). The geographic location of both study sites reveal a particular high frequency of cloud cover, making the visibility of snow cover in the satellite images limited. In this study, only images with less than 30% cloud cover were used for calibration and validation purposes. This minimizes the uncertainty of the fractional area of snow cover to less than 15% of the total investigated area as described in Glaus (2013). This restriction leads to an average of 47 days per year when snow cover images were available for the two study sites (see method section), equivalent to mean consecutive obscuration periods of ~8 days.

## MODELLING APPROACH

### The upgraded HBV model

The upgraded version of the Hydrologiska Byråns Vattenbalansavdelning model (HBV-model) is a lumped conceptual model where the watershed is represented by its fractional areas of elevation, aspect and vegetation zones and which can compute the fractional snow cover within a given catchment (Finger

*et al.*, 2015). The HBV model was originally developed by Bergström (1976, 1992) and has been widely used in Scandinavian countries and other parts of the world (Cunderlik *et al.*, 2013; Krysanova *et al.*, 1999; Razavi and Coulibaly, 2013). The upgraded HBV-light version is based on the earlier HBV-light model described in Seibert and Vis (2012) but has an upgraded glacier routine and is able to compute the major runoff components: i) snow melt ( $Q_{\text{snow}}$ ), ii) ice melt from glaciers ( $Q_{\text{ice}}$ ) and iii) rainfall runoff including rain that falls on bare ground, snow and glaciers ( $Q_{\text{rain}}$ ). Ice melting rates are computed using the degree-day method (Equation 1):

$$Q_{\text{ice}} = P_{\text{CFGlacier}} \times P_{\text{CFMAX}}(T(t) - P_{\text{TT}}) \quad (\text{Equation 1})$$

where  $P_{\text{CFMAX}}$  ( $\text{mm d}^{-1}\text{C}^{-1}$ ) is the degree-day factor and  $P_{\text{CFGlacier}}$  corrects the melt rates of ice due to lower albedo. The new features of the HBV model have successfully been tested in catchments with different degrees of glacierization (Finger *et al.*, 2015), making this model suitable for this study.

Actual evapotranspiration is calculated internally using user defined potential evapotranspiration (PET). Monthly PET was derived from observations by Einarrsson (1972) as listed in Table 1. Altogether, 21 model parameters have to be calibrated, as summarized in Table 2. A more detailed description of HBV-light can be found in Seibert and Vis (2012).

### Model application

The HBV model was set up for the respective gauged sub-catchment (River Geithellnaá gauged at station vhm149 and River Sandá gauged at station vhm026). Each watershed was divided into 100 m elevation bands, three vegetation zones (grass, wetlands and no vegetation) and north-, south- and east-west facing slopes. Additionally, in the Geithellnaá catchment, the Þrándarjökull was delineated as glacierized area and ice melt was modelled using the glacier module of the HBV-light model. As discussed by Finger *et al.* (2015) the model set up described above is adequate for runoff modelling of snow, ice and rainfall runoff.

### The multiple dataset calibration (MDC)

The HBV model was calibrated using the MDC approach (Etter *et al.*, 2017; Finger *et al.*, 2011, 2015)

combining daily satellite derived snow cover images and discharge observations of the gauged watersheds to determine the 21 model parameters. The calibration routine relies on a Monte Carlo (MC) simulation approach during which the overall consistency performance,  $P_{\text{OA}}$ , of the model is optimized.  $P_{\text{OA}}$  is an efficiency which allows equal weighting of multiple efficiency criteria as described and discussed in previous studies (Finger *et al.*, 2011, 2012, 2015). Accordingly, only a short outline of the method is presented here. First 10000 MC simulations are generated using parameter sets produced from a uniformly distributed, physically constrained, range. Out of the 10000 parameter sets, the 100 best runs for a typical one year calibration period are selected based on their performance regarding daily discharge,  $Q$ , mean monthly discharge,  $Q_{\text{monthly}}$ , and daily fractional area covered by snow,  $SC$ . Efficiency regarding daily discharge was quantified using the Nash-Sutcliffe efficiency criterion (Nash and Sutcliffe, 1970), regarding monthly mean discharge using the volumetric efficiency as suggested by Criss and Winston (2008) and regarding fractional snow cover area using the correctly predicted snow cover index (Finger *et al.*, 2015) (Table 3). Hence, the three observational datasets are only used to calibrate model parameters and there is no feedback mechanism requiring real time snow cover area as suggested by Thirel *et al.* (2012).

The year 2006 was selected as calibration period because precipitation, temperature and runoff were closest to the long-term averages in both respective watersheds. By constraining the melt parameters of the model with snow cover observations, the calibration of snow melt runoff becomes independent of geologic and pedologic characteristics, allowing a transfer of these parameters to nearby areas. The selection of the 100 best runs was made as described in Finger *et al.* (2011) by averaging the ranking values and computing an overall consistency performance,  $P_{\text{OA}}$ , regarding all efficiencies listed in Table 3. For comparison purposes the calibration routine above was repeated using only single data set calibration (namely only  $Q$ , only  $Q_{\text{monthly}}$  and only  $SC$ ) in order to assess the value of MDC.

Table 2. Overview of model parameters and their values. – *Yfirlit yfir breytur reiknilíkans.*

Parameter	<sup>(1)</sup> Description	Units	Min	Max	Vhm149		Vhm026	
					mean	std	mean	std
External groundwater contribution								
$Q_{GW}$		$m^3 s^{-1}$	0	6	0.022	-	4.74	-
Rescaling Parameters of Input Data								
$P_{PCALT}$	change of precipitation with elevation	$\% (100 m)^{-1}$	5	15	10.27	2.59	9.95	2.78
$P_{TCALT}$	change of temperature with elevation	$^{\circ}C (100 m)^{-1}$	0.5	1.5	0.95	0.25	0.84	0.20
Snow and Ice Melt Parameters								
$P_{TT}$	threshold temperature for liquid and solid precipitation.	$^{\circ}C$	-3	1	-0.88	1.01	0.37	0.48
$P_{CFMAX}$	degree-day factor	$mm d^{-1} ^{\circ}C^{-1}$	1.5	10	6.83	2.14	4.85	1.91
$P_{SFCF}$	snowfall correction factor	-	0.8	1.2	0.99	0.11	1.00	0.12
$P_{CFR}$	refreezing coefficient	-	0.02	0.1	0.06	0.02	0.05	0.02
$P_{CWH}$	water holding capacity of the snow storage	-	0.1	0.4	0.25	0.09	0.26	0.08
$P_{CFGlacier}$	glacier melt correction factor	-	0.3	3	1.70	0.80	1.82	0.77
<sup>(2)</sup> $P_{CFSlope}$	slope snow melt correction factor	-	0.3	3	1.74	0.77	1.71	0.69
<sup>(3)</sup> $P_{Kgmin}$	minimum value for the outflow coefficient representing conditions with poorly developed glacial drainage systems in late winter	-	0.01	0.2	0.11	0.05	0.11	0.06
<sup>(3)</sup> $P_{RangeKG}$	range of the annual outflow coefficient variation	-	0.01	0.5	0.29	0.13	0.26	0.14
<sup>(3)</sup> $P_{AG}$	calibration parameter defining the sensitivity of the outflow coefficient to changes in the snow storage	-	0	3	1.39	0.92	1.52	0.92
Soil Parameters								
$P_{PERC}$	maximum percolation from upper to lower groundwater storage	$mm d^{-1}$	0	4	1.49	1.02	2.29	1.09
$P_{K0}$	storage (or recession) coefficient 0	$d^{-1}$	0.1	0.5	0.37	0.09	0.30	0.11
$P_{K1}$	storage (or recession) coefficient 1	$d^{-1}$	0.01	0.2	0.13	0.05	0.13	0.05
$P_{K2}$	storage (or recession) coefficient 2	$d^{-1}$	7E-7	0.1	0.05	0.03	0.04	0.03
$P_{MAXBAS}$	length of triangular weighting function	d	1.	2.5	1.96	0.30	1.68	0.38
$P_{FC}$	Max. soil moisture storage	mm	100	700	441.46	163.54	514.41	128.68
$P_{LP}$	Rel. soil water storage below which AET is reduced linearly	-	0.3	1	0.63	0.22	0.60	0.20
$P_{Beta}$	factor governing snow and rain contribution to runoff and soil box	-	1	5	2.91	1.11	2.47	1.17

1) A detailed description of model parameters is given in Seibert and Vis (2012).

2) Slope factor correcting PCFMAX accounting for dependency of melt rates on aspect of topography.

3) Glacier parameters described in Stahl *et al.* (2008).

Particular attention was given to potential external groundwater sources as discussed in the description of the study site and described by Sigurdsson and Einarsson (1988). This was done by incorporating a new model parameter,  $Q_{GW}$ , defining an external water contribution. The unique purpose of  $Q_{GW}$  is to equilibrate the water balance of the model, but it has no further physical constraint on the ground water sys-

tem.  $Q_{GW}$  was calibrated by optimizing the overall consistency performance,  $P_{OA}$ , during MC-test runs with varying  $Q_{GW}$ . For validation purposes, the 100 best parameter sets were applied to a 10-year validation period (2001 to 2010), quantifying the efficiency of the model regarding discharge and fractional snow cover area.

Table 3. The three efficiency criteria used to evaluate model performance. – *Jöfnur reiknilíkans.*

Efficiency criteria	Calibration Period	Equation
Nash-Sutcliffe of $q^{(1)}$ , $E_Q$	1 Jan.–31 Dec.	$E_Q = 1 - \frac{\sum_{i=1}^n (q_{obs,i} - q_{sim,i})^2}{\sum_{i=1}^n (q_{obs,i} - \overline{q_{obs,i}})^2}$
Monthly volumetric efficiency of $q_{monthly}^{(1)}$ , $E_{Q,monthly}$	1 Jan.–31 Dec.	$E_{Q,monthly} = 1 - \frac{\sum_{i=1}^n (q_{monthly,obs,i} - q_{monthly,sim,i})^2}{\sum_{i=1}^n (q_{monthly,obs,i} - \overline{q_{monthly,obs,i}})^2}$
Correctly predicted snow cover area of SC <sup>(2)</sup> , $E_{SC}$	1 Jan.–31 Dec.	$E_{SC} = \frac{1}{n} \sum_{i=1}^n \left( 1 -  a_{sim,i} - a_{obs,i}  \right)$
Overall consistency performance of MDC <sup>(3)</sup> , $P_{OA}$	1 Jan.–31 Dec.	$P_{OA} = \frac{1}{3} \left( P_{E,Q} + P_{E,Q,monthly} + P_{E,SC} \right)$

Period / Area	Leirdalshraun			Heljardalsföll		
	$E_Q$	$E_{Q,monthly}$	$E_{SC}$	$E_Q$	$E_{Q,monthly}$	$E_{SC}$
Calibration (2006)	0.58	0.81	0.91	0.44	0.86	0.92
Validation (2001–2010)	0.58	0.81	0.88	0.49	0.86	0.90
Ungauged area (2001–2010)	n/a	n/a	0.89	n/a	n/a	0.89

1)  $q_{obs}$  observed daily discharge;  $q_{sim}$  is simulated daily discharge and the index  $i$  the time step.

2)  $a$  stands for the daily area fraction covered by snow; index  $sim$  and  $obs$  are estimations based on simulations or satellite images; index  $i$  is the time step and  $n$  the number of days considered.

3)  $P_{OA}$  is obtained through MDC as described in Finger *et al.* (2011).  $P_i$  is the rank value of the best MC runs regarding the efficiency  $j$ , i.e.  $E_Q$ ,  $E_{Q,monthly}$  and  $E_{SC}$ .

Finally, the 100 best parameter sets were applied to the entire hydropower exploitation area to estimate the water availability in all ungauged areas. For this purpose, HBV-light was set up for the entire hydropower area as illustrated in Figure 1a and b. Thus, assuming a power station close to the shore line at sea level, the theoretical potential energy ( $E_{pot}$  in J) of the runoff water collected in the reservoirs can be estimated considering the altitude difference between the reservoir and power station.

$$E_{pot} = V\rho gh \quad (\text{Equation 2})$$

where  $V$  is the total water volume in  $m^3$ ,  $\rho$  is the density of water in  $kg\ m^{-3}$ ,  $g$  is the gravitational constant in  $m\ s^{-2}$  and  $h$  is the altitude difference in m between reservoir and power station.

## RESULTS

### Model performance during calibration period in the gauged sub-catchments

The mean values of the model parameter sets identified during MDC are summarized in Table 2. The external groundwater contribution,  $Q_{GW}$ , converged in rivers Geithellnaá (vhm149) and Sandá (vhm026) to respective values of  $0.022\ m^3\ s^{-1}$  (equivalent to  $0.01\ mm\ d^{-1}$ ) and  $4.74\ m^3\ s^{-1}$  (equivalent to  $1.54\ mm\ d^{-1}$ ) (Figure 3a). These estimates are pure numeric values obtained by optimizing  $P_{OA}$ . Currently there are no observational data available to validate  $Q_{GW}$ . However, the estimates are comparable to results from earlier studies (Einarsson and Jónsson, 2010; Gröndal, 2002; Þórarinsdóttir, 2012) and are fortified by the annual water balance of the respective watersheds.

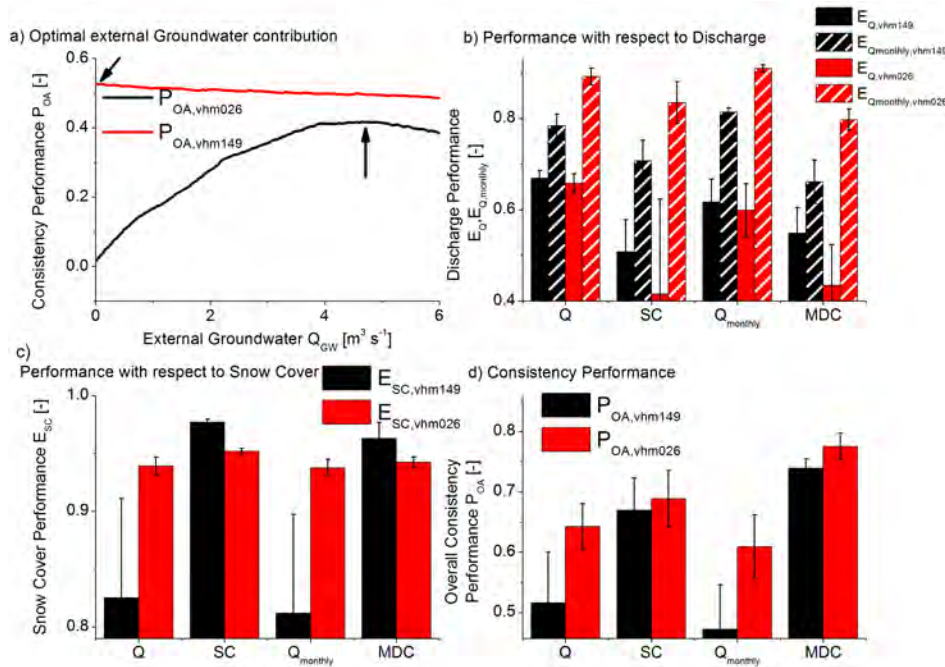


Figure 3. Model performance during calibration year 2006 in the two gauged watersheds of River Geithellnaá (vhm149) and Sandá (vhm026). Plot a) illustrates the consistency performance for 10 000 MC simulations for varying external groundwater contribution. b) and c) Mean efficiency of the 100 best runs regarding discharge and snow cover area by optimizing either for Q,  $Q_{monthly}$ , SC or applying MDC. d) Mean overall consistency performance ( $P_{OA}$ ) obtained through MDC for the 100 best MC simulations and whisker illustrate the standard deviation from the mean. – *Kvarðaðar niðurstöður gagna frá árinu 2006 fyrir mæld vatnasvæði Geithellnaár (vhm 149) og Sandár (vhm 026). a) Samleitni 10000 Monte Carlo (MC) hermana fyrir breytilegan framgang ytra grunnvatns. b) og c) Meðalnýtni 100 bestu keyrslna sem taka mið af leysingum á snjósuvæðum og hámarka Q,  $Q_{monthly}$ , SC eða nota margmiðlunarkvarðað gagnasafnskerfi (MDC). d) Meðaltal heildar samleitni ( $P_{OA}$ ) fengin með MDC fyrir 100 bestu MC hermanir, strikin gefa til kynna staðalfrávik frá meðaltali.*

The model performance of the 100 best MC simulations regarding the three efficiency criteria for the calibration period 2006 are shown in Table 3 and Figure 3, and Figure 4, for the validation period 2001 to 2010. The comparison of calibration runs using single data set calibration (optimizing only  $E_Q$ , only  $E_{SC}$  or only  $E_{Q,monthly}$ ) and all data sets combined (optimizing  $P_{OA}$ ) reveal that the individual efficiency criteria are highest when only the relevant data set is used for calibration (Figures 3b and c). However, the overall consistency performance is significantly higher when the data sets are used simultaneously for calibration (Figure 3d). The expected trade-off between MDC and efficiency performance regarding individual effi-

ciency criteria is similar to previous studies (Finger *et al.*, 2011; 2015). With mean  $E_{Q,monthly}$  above 0.8,  $E_{SC}$  above 0.9 and  $E_Q$  above 0.4 in both study sites, specific efficiencies of the MDC might appear low but are acceptable in order to assess water resources in ungauged areas on a monthly basis. This is supported by the direct comparison of observed and simulated daily and monthly discharge patterns (Figure 4) as well as snow cover ratios (Figure 5).

Figure 4a illustrates daily observed and simulated discharge patterns during the calibration year for Geithellnaá (vhm149) ranging from few  $m^3 s^{-1}$  to over  $170 m^3 s^{-1}$  ( $\sim 80 mm d^{-1}$ ). Similar patterns are observed in Sandá (at vhm026), with discharge patterns

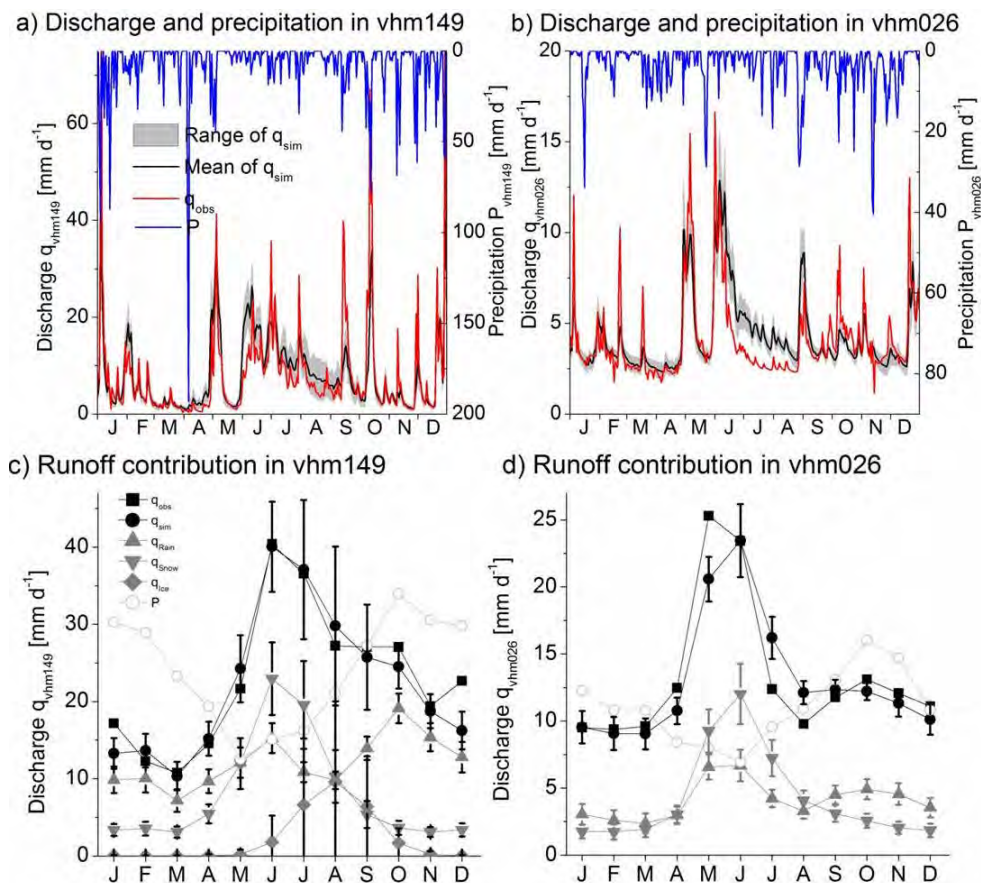


Figure 4. Daily and monthly runoff in the two gauged catchments (River Geithellnaá: vhm149 and River Sandá: vhm026). Plots a and b illustrate the mean of the MDC ( $q_{sim}$ ,  $q_{rain}$ ,  $q_{snow}$ ,  $q_{ice}$ ) and measured discharge ( $q_{obs}$ ) as well as precipitation ( $P$ ) during the calibration year (2006). Plots c and d illustrate mean monthly simulated and observed discharge for the entire validation period (2001–2010), as well as simulated rain snow and ice melt contribution. Symbols represent the monthly mean of MDC and whisker illustrate the standard deviation of the mean. – *Dag- og mánaðarlegt afrennsli á tveimur mældum vatnasvæðum (Geithellnaá: vhm 149 m og Sandá: vhm 026). a) og b) Meðaltal MDC ( $q_{sim}$ ,  $q_{rain}$ ,  $q_{snow}$ ,  $q_{ice}$ ) og mældrar leysingar ( $q_{obs}$ ) ásamt úrkomu ( $P$ ) árið 2006. c) og d) Mánaðar meðaltöl hermdrar og áætlaðrar leysingar 2001–2010 ásamt hermdri úrkomu, snjó og ísbráðnun. Tákn gefa til kynna mánaðarleg meðaltöl MDC ásamt staðalfrávikum.*

varying up to  $50 \text{ m}^3 \text{ s}^{-1}$  ( $>15 \text{ mm d}^{-1}$ ) within a few days, revealing a very dynamic runoff (Figure 4b). It is noticeable that observed and simulated daily runoff at vhm026 remains above  $4.7 \text{ m}^3 \text{ s}^{-1}$  ( $1.5 \text{ mm d}^{-1}$ ), revealing the continuous contribution of groundwater inflow, dominating the discharge during the cold winter months. Besides some short-term discrepancies during summer floods, the daily patterns are generally

well reproduced by the model and comparable with earlier studies (Einarsson and Jónsson, 2010; Gröndal, 2002; Þórarinsdóttir, 2012).

#### Model performance during the 10-year validation period

In Figure 4c and d, simulated and observed mean monthly discharge of the two gauging stations (vhm149 and vhm026) is illustrated for the entire 10-

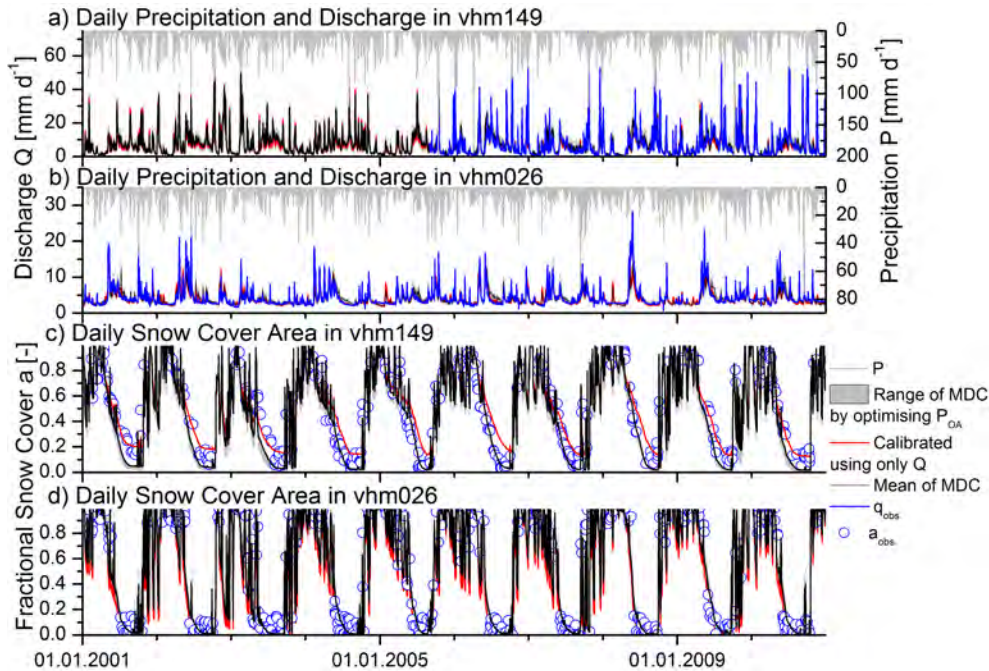


Figure 5. Daily discharge and fractional snow cover obtained with MDC and optimizing for  $Q$  only in the gauged watershed of Geithellnaá (at station vhm149) and Sandá (at station vhm026) during the validation period (2001–2010). Panels a and b illustrate simulated and observed daily discharge rates. Panels c and d illustrate simulated and observed daily fractional snow cover ratios. The grey area (range of  $a_{sim}$  and  $q_{sim}$ ) and the black line (mean of  $a_{sim}$  and  $q_{sim}$ ) indicate the range of MDC by optimizing  $P_{OA}$ , the red line indicates the performance if only  $Q(a_{sim,eq}$  and  $q_{sim,eq})$  was used for calibration and the blue line and symbols illustrate observations. – MDC meðaltal daglegrar leysingar og hlutfallslegrar snjóþekju, hámarks- og lágmarks- og meðaltal af  $a_{sim}$  og  $q_{sim}$  fyrir  $Q$  á mældu vatnasvæði Geithellnaár (vhm 149) og Sandár (vhm 026), tímabilið 2001–2010. a) og b) Hermdur og áætlaður daglegur hraði leysingar. c) og d) Hermt og áætlað snjóþekjuhutfall. Gráa svæðið ( $a_{sim}$  og  $q_{sim}$ ) og svarta línan (meðaltal af  $a_{sim}$  og  $q_{sim}$ ) sýna MDC með því að hámarka  $P_{OA}$ . Rauða línan; niðurstöður ef aðeins  $Q(a_{sim,eq}$  og  $q_{sim,eq})$  voru notuð til kvörðunar, bláa línan og tákn sýna athuganir.

year validation period (2001 to 2010, excluding the missing data period between the end of 2001 and the beginning of 2006 for vhm149, e.g. River Geithellnaá) using the parameter sets determined during the calibration period. Overall, the monthly means are well reproduced (mean  $E_{Q,monthly} = 0.81$  for vhm149 and 0.86 for vhm026; Figure 4c and d), indicating that the calibration approach is suitable for season discharge simulations.

Daily discharge and snow cover ratios in both study sites are illustrated in Figure 5. The simulated and observed daily discharge patterns reveal some discrepancies but correspond generally well throughout the entire validation period (mean  $E_Q = 0.58$  for

vhm149 and 0.49 for vhm026) in both gauged catchments (Figure 5a and b). MDC reveals almost identical daily discharge patterns as the single dataset calibration optimizing only  $E_Q$ . This indicates that the one-year calibration period is sufficient to generate daily discharge patterns during the entire 10 year validation period, agreeing with previous studies (Finger *et al.*, 2011, 2012, 2015). Simulated and observed fractional snow cover area is well reproduced throughout the entire validation period (mean  $E_{SC} = 0.89$  for vhm149 and 0.90 for vhm026) in both catchments (Figure 5c and d). It is noticeable that the calibration optimizing  $E_Q$  leads to significant overestimation of snow cover in the area in the drainage area

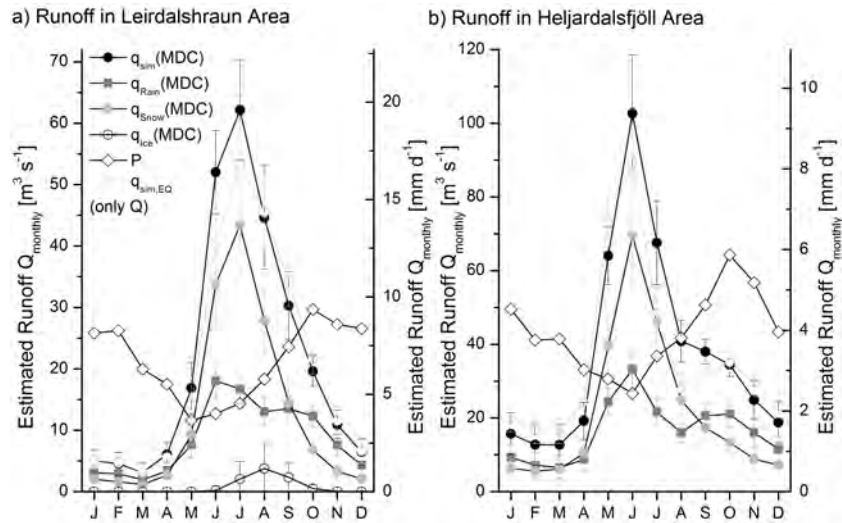


Figure 6. Estimated water amount ( $q_{sim}$ ) available for hydropower production in Leirdalshraun (a) and Heljardalsfjöll area (b) and the contribution of snow ( $q_{Snow}$ ) and ice melt ( $q_{Ice}$ ), rainfall runoff ( $q_{Rain}$ ), as well as precipitation ( $P$ ) during the period 2001–2010. All results are based on MDC, except  $q_{sim,EQ}$  which is obtained by using only  $Q$  for calibration. Symbols represent the monthly mean of MDC and whisker illustrate the standard deviation of the mean. – Áætlað nýtanlegt vatnsmagn ( $q_{sim}$ ) til vatnsaflsframleiðslu í Leirdalshrauni (a) og svæði Heljardalsfjalla (b) vegna snjóa ( $q_{Snow}$ ), ísbráðnunar ( $q_{Ice}$ ) affallsvatns ( $q_{Rain}$ ) og úrkomu ( $P$ ) fyrir tímabilið 2001–2010. Allar niðurstöður eru byggðar á MDC, nema  $q_{sim,EQ}$  sem er kvarðað út frá  $Q$ . Tákn gefa til kynna mánaðarlegt meðaltal MDC og strik staðalfrávik frá meðaltali.

of vhm149 during all summer months of the calibration period. This effect is less visible in the drainage area of vhm026, revealing lower performance regarding snow cover area during numerous individual days.

During winter months both watersheds are entirely covered by snow as average temperatures are below freezing. During summer from August until mid-October, the Sandá watershed (vhm026) is nearly snow free, while snow cover in the Geithellnaá watershed (vhm149) can account for up to 5% of the area in some years. Overall the simulated discharge (Figure 5a and b) and snow cover area (Figure 5c and d) do not reveal any major discrepancies during the validation period, indicating an adequate and consistent calibration of the model.

#### Estimations of runoff in the ungauged area

In order to estimate total available runoff in the ungauged area, the parameter sets identified during the calibration period were applied to a model comprising the entire area designated for hydropower exploitation

(Figure 1). The simulated monthly discharge between 2001 and 2010 from the ungauged areas, Leirdalshraun and Heljardalsfjöll, is illustrated in Figure 6.

In Leirdalshraun, monthly runoff is estimated to be less than  $5 \text{ m}^3 \text{ s}^{-1}$  during the winter months but exceeding  $50 \text{ m}^3 \text{ s}^{-1}$  during the summer months. 57% of the total runoff is attributed to snow melt, while the remaining discharge can be attributed to rainfall runoff and ice melt from Þrándarjökull, the latter accounting for less than 4% of the total runoff (Figure 6a).

In the Heljardalsfjöll area, monthly runoff drops below  $15 \text{ m}^3 \text{ s}^{-1}$  during the winter months and reaches over  $90 \text{ m}^3 \text{ s}^{-1}$  during the month of July (Figure 6b). Similarly to Leirdalshraun, ~57% of the total runoff is attributed to snow melt.

It is noticeable that in both areas the calibration optimizing  $E_Q$  leads to significantly lower runoff during the summer month than estimations based on optimizing  $P_{OA}$  (Figure 6). Since no discharge data exist, it is impossible to state which estimation is more re-

alistic. Nevertheless, the advantages of MDC by optimizing  $P_{OA}$  are convincing, as outlined in the discussion section of this paper.

As snow melt in both areas accounts for more than half of the total runoff (Figure 6) it can be argued that an adequate simulation of snow cover is a good indicator for a robust and realistic runoff estimation. In Figure 7, the simulated fraction of snow cover in the Leirdalshraun and Heljardalsfjöll areas is compared to the observations in satellite snow cover images. While Heljardalsfjöll is almost completely snow free every summer, about 20 % of Leirdalshraun remains snow covered during the entire summer. The simulated snow cover obtained by optimizing  $P_{OA}$  matches the snow cover fraction determined in satellite pictures adequately (mean  $E_{SC} = 0.88$  for Leirdalshraun and 0.89 for Heljardalsfjöll; Table 3). Simulated snow cover area obtained by optimizing  $E_Q$  leads to significant discrepancy, overestimating snow cover in Leirdalshraun by up to 30% during all summer months and underestimating snow cover in Heljardalsfjöll during numerous days. MDC reveals significantly better performance, indicating that the observed snow cover area is most of the time within the standard deviation of the mean of the 100 best MC runs. Regarding the reasonable model performance in the gauged catchments of rivers Geithellnaá and Sandá (vhm149 and vhm026) and the adequate performance of simulated snow cover in the ungauged areas, the runoff estimations for the ungauged areas using MDC can be considered the most reasonable estimations with currently available information.

### Estimations of the hydropower potential of the ungauged areas

Based on the modelling results, the total water availability in the form of liquid and solid precipitation and ice melt in the two study areas amounts to 1880 million  $m^3$  water annually (Table 4). Under the assumption that the entire water of the two study sites is deviated into the respective reservoirs  $R_L$  and  $R_H$  located at elevation of 595 m a.s.l. (Leirdalshraun) and 235 m a.s.l. (Heljardalsfjöll), the potential energy,  $E_{pot}$ , of this water can be estimated using classical mechanics (Equation 2). In Figure 8, monthly  $E_{pot}$  is illustrated accounting for the total elevation differ-

ence between sea level (0 m a.s.l.) and the respective reservoirs.  $E_{pot}$  of the annual water collected in the two hypothetical reservoirs ( $R_L$  and  $R_H$ ) accounts for 1.8 TWh  $a^{-1}$ . In order to transform this energy into usable electric energy the collected water would need to be delivered through pressure pipelines to conventional Pelton turbines close to sea-level. The efficient exploitation and transformation of  $E_{pot}$  represent a challenging task, as various aspects (e.g. inter annually changing reservoir elevation, number of turbines, and length of waterways) have to be accounted for in order to maximize the overall efficiency of the power plant. A complete description of the power plant would go beyond the objective of this study. Typical overall plant efficiency ranges between 0.5 and 0.95 (Zhou *et al.*, 2015). Hence, assuming a very conservative overall efficiency of 0.6 the estimated electric energy production in the two study sites could amount up to 1.1 TWh  $a^{-1}$  (665 GWh  $a^{-1}$  in Leirdalshraun and 452 GWh  $a^{-1}$  in Heljardalsfjöll). However, besides the steep and inaccessible terrain of the two ungauged catchments, the highly dynamic discharge patterns present an additional challenge to install hydropower infrastructure in this remote mountain area.

Table 4. Summary of catchment characteristics and potential for energy production for Leirdalshraun (L) and Heljardalsfjöll (H). – *Áætlað vatnsmagn til vatnsaflsframleiðslu á vatnasviðum Leirdalshrauns og Heljardalsfjalla.*

	Unit	L	H
Total area	km <sup>2</sup>	274	946
Glacierization	%	5	0
Total precipitation P	mm a <sup>-1</sup>	2441	1441
	m <sup>3</sup> s <sup>-1</sup>	21.2	43.2
Simulated water availability $Q_{sim}$	m <sup>3</sup> s <sup>-1</sup>	21.8	37.6
	M m <sup>3</sup> a <sup>-1</sup>	691.5±10.3	1190.5±17.5
50 % quantile $Q_{50}$	m <sup>3</sup> s <sup>-1</sup>	7.1	18.3
5 yr return period $T_5$	m <sup>3</sup> s <sup>-1</sup>	174	373
Altitude difference $\Delta h$	m	Max595	Max235
Pot. energy $E_{pot}$	GWh a <sup>-1</sup>	~1121	~762
Overall efficiency <sup>(1)</sup>	–	0.6	0.6
Hydropower	GWh a <sup>-1</sup>	~665	~452
Potential <sup>(1)</sup> P			

(1) The overall efficiency of a typical hydropower plant ranges between 0.5 and 0.95 (Zhou *et al.*, 2015). Here a conservative efficiency of 0.6 was assumed.

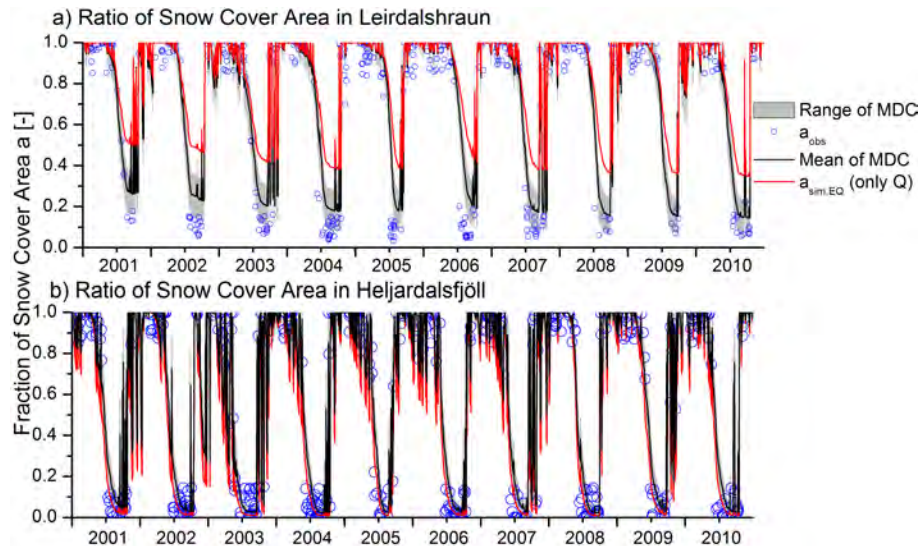


Figure 7. Validation of the fractional snow cover area in the ungauged Leirdalshraun and the Heljardalsfjöll areas during the 10 year validation period (2001 to 2010). All results are based on MDC by optimizing  $P_{OA}$ , except  $a_{sim,EQ}$  which is obtained by calibration only against  $Q$ . – Staðfesting á hlutfallslegu snjóþekjusvæði í ómældu Leirdalshrauni og á Heljardalsfjallasvæði yfir 10 ára tímabil frá (2001–2010). Allar niðurstöður eru byggðar á MDC með því að hámarka  $P_{OA}$ , nema  $a_{sim,EQ}$  sem er fengið með kvörðun út frá  $Q$ .

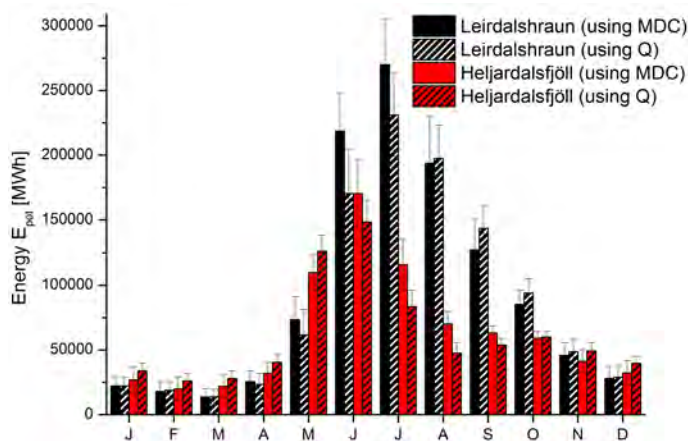


Figure 8: Estimated potential energy from the estimated runoff in Leirdalshraun and the Heljardalsfjöll area. Results are based on MDC by optimizing  $P_{OA}$  or calibrating only against  $Q$ , as indicated in the legend. – Mynd 8. Áætluð stöðuorka frá áætluðu afrennslisvatni í Leirdalshrauni og svæðum Heljardalsfjalla. Niðurstöðurnar eru byggðar á MDC með því að hámarka  $P_{OA}$  eða kvarða fyrir  $Q$  eins og sýnt er í skýringum.

## DISCUSSION

The estimations of runoff in ungauged catchments is a core challenge of hydrological research. In the past most researchers regionalized model parameters, arguing that similar catchment characteristics (e.g. sizes of the basins, topography, elevation, snow cover area, geology, precipitation, soil type, soil cover) justify a transfer of calibrated model parameters to un-

gauged watersheds (Merz and Blöschl, 2004; Sefton and Howarth, 1998; Seibert, 1999). However, in mountain catchments and volcanic areas characterized by direct snow and ice melt runoff and faults in the bedrock (e.g. porous lava fields or karst systems) a regionalization can become inadequate as it might misrepresent local characteristics. This paper presents a supplement to the regionalization method

by demonstrating the value of MDC, using namely satellite retrieved snow cover and daily discharge observations to enhance the overall consistency performance of the model (Finger *et al.*, 2015). More importantly, the presented results show how remotely sensed snow cover data can be used to validate the snow cover. This is especially valuable in catchments dominated by snow melt, as a realistic simulation of snow cover implies adequate snow melt rates.

The results presented for the two case studies in Iceland reveal that the combination of snow cover images and discharge patterns can significantly improve the overall consistency performance (Figure 3d), as defined in (Finger *et al.*, 2015). While MDC reveals slightly lower Nash-Sutcliffe efficiencies (Figure 3b), MDC leads to drastically better  $E_{SC,monthly}$  performance (Figure 3c) and significantly better  $P_{OA}$  (Figure 3d) than calibration using only discharge data. In particular, MDC can be used to estimate an external groundwater,  $Q_{GW}$ , contribution (Figure 3a), balancing out the water budget of complex watersheds. For both case studies the optimization of  $P_{OA}$  leads to a realistic  $Q_{GW}$  estimation, falling in line with previous studies (Einarsson and Jónsson, 2010; Gröndal, 2002; Þórarinsdóttir, 2012). The determination of an external groundwater contribution implies that the main water sources, e.g. snow melt and ice melt, are realistically estimated. Accordingly, an enhanced overall consistency performance, as illustrated in Figure 3d, is essential to avoid unrealistic trade-offs between water sources. Nevertheless, the determined  $Q_{GW}$  remains an estimate and would require extensive tracer experiments to be validated (Finger *et al.*, 2013).

MDC leads inevitably to a reduction of individual efficiencies, as multiple objective optimization is always linked to a trade-off between the considered efficiencies (Figure 3, Table 3). However, daily discharge and snow cover area for the gauged catchments reveals to be reproduced adequately for the entire 10-year validation period (Figure 5). In contrast to this performance calibration using only discharge data leads to significant discrepancies of simulated snow cover area (Figure 5c and d), revealing the poor consistency of the simulations based on calibration using only discharge data (Figure 3d).

The simulations using MDC are suitable to estimate seasonal patterns of runoff and the contribution of snow melt in the area as observations are most of the time within modelling uncertainty (Figure 6). The simulation results indicate that in gauged rivers snow melt contributes more than half of the water to the total runoff (Figure 6a,b). Accordingly, adequate snow cover simulations are essential to make estimations of runoff in ungauged areas realistic. The presented results reveal that simulated seasonal snow cover corresponds well (mean  $E_{SC} = 0.88$  for Leirdalshraun and 0.89 for Heljardalsfjöll) to the available snow cover images in both ungauged areas (Figure 7). Contrastingly, simulations obtained by calibrating only with  $Q$ , significantly overestimate snow cover area in Leirdalshraun and reveal numerous discrepancies from observation in Heljardalsfjöll. The results reveal also that snow cover in both areas evolves gradually (Figure 7), making weekly satellite images sufficient for calibration purposes. Accordingly, MODIS daily snow cover products are suitable for model calibration and validation, despite the frequent cloud cover in Iceland (on average only 47 cloud free images per year were available between 2001 and 2010, resulting in mean obscuration periods of 8 days). By using the daily product rather than the 8 day composite MODIS product, the timing of a change in snow cover status for single cells can be accounted for more precisely, as also discussed by Finger *et al.* (2011, 2012 and 2015). Based on the discussion above, the total estimated runoff from both ungauged areas and the associated hydropower potential obtained using MDC appear to be the best possible estimation with the currently available data. As illustrated in Figure 8, results from calibration using only  $Q$  differ significantly from results obtained with MDC, revealing the importance of MDC for ungauged mountain areas.

Nevertheless, the presented estimations are subject to various uncertainties, which should be considered carefully before using the results for further purposes. The presented runoff estimations rely on only 10 years of data availability, and might not adequately account for the frequency of extreme dry or wet years. Furthermore, the overall efficiency of hydroelectricity plants ranges between 0.5 and 0.95

(Zhou *et al.*, 2015). In this study a conservative efficiency of 0.6 was assumed which has also been reported in other power plants in arctic regions (Hartmann *et al.*, 2017). It is therefore strongly advisable to collect additional field data before using the present estimates for decisions regarding the development of water infrastructure. In particular the following field observations should be collected to provide additional validation of the estimations: i) tracer experiments to determine external ground water contribution (Finger *et al.*, 2013), ii) detailed assessment of the water balance with additional discharge and precipitation observations, iii) experimental observation of precipitation and temperature gradients to validate gridded weather input data and iv) snow depth and glacier mass balances in order to validate snow and ice contribution. While these additional datasets would certainly fortify the results, the presented estimations are the best possible estimates for data scarce areas and very probably are more realistic than estimates based on calibration using only  $Q$ .

Last but not least, the presented figures are based on 100% efficient water collection in the two catchments. However, the terrain in both areas is steep, inaccessible and partially highly erodible. Accordingly, the installation of infrastructure to collect runoff water from ungauged catchments presents a compelling civil engineering challenge. Furthermore, the high runoff dynamic due to the local weather patterns present an additional challenge to effectively harvest all the water available in the two watersheds.

Considering all of the concerns addressed above, the modelling results should be interpreted as a realistic first estimate of water runoff in the ungauged areas. Since snow cover images derived from the MODIS product are available for the entire world, the presented approach can be applied to any watershed worldwide, making it also suitable for large scale modelling.

## CONCLUSIONS

The conceptual hydrological model HBV was calibrated using a multi dataset calibration (MDC) technique, based on discharge and daily satellite snow cover images for gauged sub-catchments of potential areas designated for future hydropower reservoirs.

The calibrated model was applied to the hydropower exploitation area defined by Orkustofnun for potential hydropower use. With this method, the total hydropower potential for the entire area, including ungauged catchment, was estimated. Based on the presented results the following conclusion can be drawn:

The combination of discharge data and snow cover images allows a realistic estimate of external ground water contribution,  $Q_{GW}$ , balancing the water budget of complex watersheds. For the two gauged watersheds, River Geithellnaá (vhm149) and Sandá (vhm026),  $Q_{GW}$  was estimated to amount up to 0.022 and  $4.74 \text{ m}^3 \text{ s}^{-1}$ , respectively, falling in line with previous studies (Einarsson and Jónsson, 2010; Gröndal, 2002; Þórarinsdóttir, 2012). This is an essential finding to estimate total runoff in the two ungauged areas.

The complementary use of satellite retrieved snow cover images and one year of discharge observations to calibrate a hydrological model reveals that snow melt can be adequately predicted in ungauged mountain areas. This technique allows improving and validating estimations of water resources in mountain areas with limited data availability.

The subpolar location of Iceland leads to frequent cloud cover limiting the use of satellite imaging. On average only 47 snow cover maps per year were available. Nevertheless, the presented results reveal that despite the frequent cloud cover, satellite retrieved snow cover images improve model performance significantly and are suitable for the validation of snow cover and snow melt in ungauged areas.

In the Leirdalshraun area, the total volume of annual melt and rain water is estimated up to 691 million  $\text{m}^3$  of water. This water could be collected and stored in a reservoir at an altitude of 595 m a.s.l.. Accordingly, the potential energy accounts up to  $1121 \text{ GWh a}^{-1}$ , which could result in an annual energy production of up to 665 GWh of hydroelectricity.

In the Heljardalsfjöll area, the total volume of melt and rain water is estimated up to 1191 million  $\text{m}^3$  of water. This water could be collected and stored in a reservoir at an altitude of 235 m a.s.l.. Accordingly, the potential energy accounts up to  $762 \text{ GWh a}^{-1}$ , which could result in an annual energy production of up to 452 GWh of hydroelectricity.

Altogether, the total estimated hydropower potential of the two watersheds combined amounts up to 1.1 TWh a<sup>-1</sup>, which represents about 10% of Iceland's current energy production. Nevertheless, these numbers have to be considered with precaution, as they are based on a number of assumptions (see discussion section) and on 100% efficient water harvesting in the area, which presents a compelling civil engineering challenge.

Finally, the use of daily snow cover images in combination with limited discharge observations are a valuable modelling approach that can be applied worldwide, allowing a realistic estimation of water resources in ungauged mountain areas.

### Acknowledgments

This study was funded by Orkustofnun (National Energy Authority of Iceland, NEA). Digital elevation maps were provided by the Icelandic Geodetic Survey and discharge data by the Icelandic Meteorological Office (IMO). Land cover maps were obtained from the CORINE programme of the European Environmental Agency (EEA). MODIS snow cover images were obtained from the National Snow and Ice Data Center (NSIDC). Philippe Crochet (IMO) provided gridded meteorological data. The outlines of the potential hydropower area (as illustrated in Figures 1 and 3) have been defined in joint discussion with Kristinn Einarsson and Linda Georgsdóttir (both NEA). Two anonymous reviewers gave valuable recommendations to an earlier version of this manuscript. Special thanks go to Jens Arnljótsson for the Icelandic translation.

### ÁGRIP

Við gerð stefnumótunar um stjórnun endurnýjanlegs vatnsafls er mikilvægt að leggja mat á nýtanlegt vatns-magn á ómældum svæðum. Vatnafræðileg líkön eru öflug tæki við að greina vatna- og veðurfarsleg gögn og áætla heildarmagn vatns frá ómældum svæðum. Gervitunglamyndir gefa mikilvægar upplýsingar um snjómagn á fjallasvæðum. Hydrologiska Byråns Vattenbalansavdelning model (HBV) var notað til að áætla heildarmagn af snjó og afrennslisvatni á tveimur ómældum svæðum á norðaustanverðu Íslandi (Leirdalshrauni, 274 km<sup>2</sup> yfir 595 m.y.s. og Heljardals-

fjöllum 946 km<sup>2</sup> yfir 235 m.y.s.). Þetta vatns-magn mætti hugsanlega nýta til vatnsaflsvirkunar. Breyt-urnar í líkaninu voru ákvarðaðar með margmiðlun-arkvörðuðu gagnasafnskerfi (MDC) sem byggði á árs upplýsingum frá gervitunglamyndum af snjóþekju og skráðum gögnum um leysingar af mældum undir-vatnasvæðum. Með því að nota fyrrnefndar líkana-breytur er hægt að áætla hve mikið vatnsafl er hægt að nýta frá ómældum svæðum. Snjóþekjur á ómældum svæðum ásamt leysingarvatni af mældum vatnasvæð-um var metið yfir 10 ára tímabil og kom í ljós mik-il bráðnun á öllu svæðinu. Heildarmagn vatns vegna bráðunar á ís og snjó, ásamt regni og afrennslisvatni var ca. 690 M m<sup>3</sup>/ári í Leirdalshrauni og 1190 M m<sup>3</sup>/ári í Heljardalsfjöllum. Fræðileg stöðuorka þess-ara vatnsorkulinda er nálægt 1,9 TWh/ári sem er feiki-lega mikið og beisla mætti með uppistöðulóni og leiða í hverfla til vatnsaflsvirkunar við sjávarmál. Þó að niðurstöðurnar séu aðeins gildar fyrir ákveðið tilvik þá er hægt að beita líkaninu á önnur fjalllend svæði.

### REFERENCES

- Adler, R.F., G.J. Huffman, A. Chang, R. Ferraro, P.P. Xie, J. Janowiak, B. Rudolf, U. Schneider, S. Curtis, D. Bolvin, A. Gruber, J. Susskind, P. Arkin and E. Nelkin 2003. The version-2 global precipitation climatology project (GPCP) monthly precipitation analysis (1979-present). *J. Hydrometeorol.* 4(6), 1147–1167, doi:10.1175/1525-7541(2003)-004<1147:tvGPCP>2.0.co;2
- Bergström, S. 1976. *Development and application of a conceptual runoff model for Scandinavian catchments*. Swedish Meteorological and Hydrological Institute SMHI Report RHO 7, 134 pp. Norrköping.
- Bergström, S. 1992. *The HBV model – its structure and applications*. Swedish Meteorological and Hydrological Institute (SMHI), Report RH4, 35 pp., Norrköping.
- Björnsson, H., F. Palsson, S. Gudmundsson, E. Magnusson, G. Adalgeirsdóttir, T. Johannesson, E. Berthier, O. Sigurdsson and Th. Thorsteinsson 2013. Contribution of Icelandic ice caps to sea level rise: Trends and variability since the Little Ice Age. *Geophys. Res. Lett.* 40(8), 1546–1550, doi:10.1002/grl.50278
- Brakenridge, G.R., S. Cohen, A.J. Kettner, T. De Groeve, S. V. Nghiem, J.P.M. Syvitski and B.M. Fekete 2012. Calibration of satellite measurements of river discharge using a global hydrology model. *J. Hydrology* 475, 123–136, doi:10.1016/j.jhydrol.2012.09.035
- Coxon, G., J. Freer, I.K. Westerberg, T. Wagener, R. Woods and P.J. Smith 2015. A novel framework for discharge uncertainty quantification applied to 500 UK gaug-

- ing stations. *Water Resources Res.* 51(7), 5531–5546, doi:10.1002/2014wr016532
- Criss, R. E. and W. E. Winston 2008. Do Nash values have value? Discussion and alternate proposals. *Hydrol. Proc.* 22(14), 2723–2725, doi:10.1002/hyp.7072
- Crochet, P. and T. Johannesson 2011. A data set of gridded daily temperature in Iceland, 1949–2010. *Jökull* 61, 1–18.
- Crochet, P., T. Johannesson, T. Jonsson, O. Sigurdsson, H. Björnsson, F. Pálsson and I. Barstad 2007. Estimating the spatial distribution of precipitation in Iceland using a linear model of orographic precipitation. *J. Hydrometeorol.* 8(6), 1285–1306, doi:10.1175/2007jhm795.1
- Cunderlik, J. M., S. W. Fleming, R. W. Jenkinson, M. Thiemann, N. Kouwen and M. Quick 2013. Integrating logistical and technical criteria into a multiteam, competitive watershed model ranking procedure. *J. Hydrol. Eng.* 18(6), 641–654, doi:10.1061/(asce)he.1943-5584.0000670
- Dong, J. R., J. P. Walker and P. R. Houser 2005. Factors affecting remotely sensed snow water equivalent uncertainty. *Remote Sensing Env.* 97(1), 68–82, doi:10.1016/j.rse.2005.04.010
- Duethmann, D., J. Peters, T. Blume, S. Vorogushyn and A. Guntner 2014. The value of satellite-derived snow cover images for calibrating a hydrological model in snow-dominated catchments in Central Asia. *Water Resources Res.* 50(3), 2002–2021, doi:10.1002/2013wr014382
- Egilson, D. and G. Stefánsdóttir 2014. *Álagsþættir á grunvatn*. Report DE/GSt/2014-01, 31 pp. The Icelandic Meteorological Office, Reykjavík.
- Einarsson, B. and S. Jónsson 2010. Improving groundwater representation and the parameterization of glacial melting and evapotranspiration in applications of the WaSiM hydrological model within Iceland. Report VI2010-016, 29 pp. The Icelandic Meteorological Office, Reykjavík.
- Einarsson, M. 1972. *Evaporation and potential evaporation in Iceland*. 14 pp. The Icelandic Meteorological Office, Reykjavík.
- Einarsson, P. 2008. Plate boundaries, rifts and transforms in Iceland. *Jökull* 58, 35–58.
- El Maayar, M. and J. M. Chen 2006. Spatial scaling of evapotranspiration as affected by heterogeneities in vegetation, topography, and soil texture. *Remote Sensing Env.* 102(1–2), 33–51, doi:10.1016/j.rse.2006.01.017
- Etter, S., N. Addor, M. Huss and D. Finger 2017. Climate change impacts on future snow, ice and rain runoff in a Swiss mountain catchment using multi-dataset calibration. *J. Hydrology-Regional Studies* 13, 222–239, doi:10.1016/j.ejrh.2017.08.005
- Finger, D., G. Heinrich, A. Gobiet and A. Bauder 2012. Projections of future water resources and their uncertainty in a glacierized catchment in the Swiss Alps and the subsequent effects on hydropower production during the 21st century. *Water Resources Res.* 48, doi:10.1029/2011wr010733, W02521.
- Finger, D., A. Hugentobler, M. Huss, A. Voinesco, H. R. Wernli, D. Fischer, E. Weber, P.-Y. Jeannin, M. Kauzlaric, A. Wirz, T. Vennemann, F. Hüsler, B. Schädler and R. Weingartner 2013. Identification of glacial melt water runoff in a karstic environment and its implication for present and future water availability. *Hydrol. Earth System Sci.* 17, 3261–3277, doi:10.5194/hess-17-3261-2013
- Finger, D., F. Pellicciotti, M. Konz, S. Rimkus and P. Burlando 2011. The value of glacier mass balance, satellite snow cover images, and hourly discharge for improving the performance of a physically based distributed hydrological model. *Water Resources Res.* 47, doi:10.1029/2010wr009824, W07519.
- Finger, D., M. Vis, M. Huss and J. Seibert 2015. The value of multiple data set calibration versus model complexity for improving the performance of hydrological models in mountain catchments. *Water Resources Res.* 51, 1939–1958, doi:10.1002/2014wr015712
- Gislason, S. R. 2008. Weathering in Iceland. *Jökull* 58, 387–408.
- Glaus, N. 2013. *Snow Cover in the vicinity of Glacier de la Plaine Morte*. BSc. Thesis, 103 pp. University of Bern, Switzerland.
- Gröndal, G. O. 2002. *Sandá í Þistilfirði. Gerð HBV-rennsliðskans af vhm 026*. Report OS-2002/036, 32 pp. Orkustofnun, Vatnamælingar.
- Gupta, H. V., C. Perrin, G. Bloschl, A. Montanari, R. Kumar, M. Clark and V. Andreassian 2014. Large-sample hydrology: a need to balance depth with breadth. *Hydrol. Earth System Sci.* 18(2), 463–477, doi:10.5194/hess-18-463-2014
- Hall, D. K., G. A. Riggs, J. L. Foster and S. V. Kumar 2010. Development and evaluation of a cloud-gap-filled MODIS daily snow-cover product. *Remote Sensing Env.* 114(3), 496–503, doi:10.1016/j.rse.2009.10.007
- Hall, D. K., G. A. Riggs, V. V. Salomonson, N. E. DiGirolamo and K. J. Bayr 2002. MODIS snow-cover products. *Remote Sensing Env.* 83(1–2), 181–194, doi:10.1016/s0034-4257(02)00095-0
- Hartmann, J., B. Rydgrenand and E. Taylor-Wood 2017. *Kárahnjúkar Hydropower Project*. 166 pp. Landsvirkjun, Sweco, Entura, Reykjavík, Iceland.
- Hock, R. 2005. Glacier melt: a review of processes and their modelling. *Progress in Physical Geography* 29(3), 362–391, doi:10.1191/0309133305pp453ra
- Jeannin, P. Y., U. Eichenberger, M. Sinreich, J. Vouillamoz, A. Malard and E. Weber 2013. KARSYS: a pragmatic approach to karst hydrogeological system conceptualisation. Assessment of groundwater reserves and resources in Switzerland. *Env. Earth Sci.* 69(3), 999–1013, doi:10.1007/s12665-012-1983-6
- Jonsdóttir, J. F. 2008. A runoff map based on numerically simulated precipitation and a projection of future runoff in Iceland. *Hydrological Sci. J.* 53(1), 100–111, doi:10.1623/hysj.53.1.100
- Jost, G., R. D. Moore, R. Smith and D. R. Gluns 2012. Distributed temperature-index snowmelt modelling for forested catchments. *J. Hydrology* 420, 87–101, doi:10.1016/j.jhydrol.2011.11.045.
- Khan, S. I., Y. Hong, J. H. Wang, K. K. Yilmaz, J. J. Gourley, R. F. Adler, G. R. Brakenridge, F. Policelli, S. Habib and D. Irwin 2011. Satellite remote sensing and hydrologic modeling for flood inundation mapping in Lake Victoria Basin:

- Implications for hydrologic prediction in ungauged basins. *IEEE Trans. Geoscience and Remote Sensing* 49(1), 85–95, doi:10.1109/tgrs.2010.2057513
- Koboltschnig, G.R., W. Schoener, M. Zappa, C. Kroisleitner and H. Holzmann 2008. Runoff modelling of the glacierized Alpine Upper Salzach basin (Austria): multi-criteria result validation. *Hydrol. Proc.* 22(19), 3950–3964, doi:10.1002/hyp.7112
- Krysanova, V., A. Bronstert and D.I. Muller-Wohlfeil 1999. Modelling river discharge for large drainage basins: from lumped to distributed approach. *Hydrol. Sci. J.* 44(2), 313–331, doi:10.1080/02626669909492224
- Lamouroux, N., H. Pella, T.H. Snelder, E. Sauquet, J. Lejot and U. Shankar 2014. Uncertainty models for estimates of physical characteristics of river segments over large areas. *J. Am. Water Res. Ass.* 50(1), 1–13, doi:10.1111/jawr.12101
- McMillan, H., A. Montanari, C. Cudennec, H. Savenije, H. Kreibich, et al. 2016. Panta Rhei 2013–2015: Global perspectives on hydrology, society and change. *Hydrol. Sci. J.* 61(7), 1174–1191. doi:10.1080/02626667.2016.1159308
- Merz, R. and G. Bloschl 2004. Regionalisation of catchment model parameters. *J. Hydrology* 287(1-4), 95–123, doi:10.1016/j.jhydrol.2003.09.028
- Moss, D. and B.K. Wyatt 1994. The CORINE Biotopes project – a database for conservation of nature and wildlife in the European-Community. *Appl. Geography* 14(4), 327–349, doi:10.1016/0143-6228(94)90026-4
- Nash, J.E. and J.V. Sutcliffe 1970. River flow forecasting through conceptual models Part 1 - A discussion of principles. *J. Hydrology* 10, 282–290,
- Orkustofnun 2014. *Energy statistics in Iceland*. 14 pp. Orkustofnun, Reykjavík.
- Pechlivanidis, I.G. and B. Arheimer 2015. Large-scale hydrological modelling by using modified PUB recommendations: the India-HYPE case. *Hydrol. Earth System Sci.* 19(11), 4559–4579, doi:10.5194/hess-19-4559-2015
- Razavi, T. and P. Coulibaly 2013. Streamflow prediction in ungauged basins: Review of regionalization methods. *J. Hydrol. Eng.* 18(8), 958–975, doi:10.1061/(asce)he1943-5584-0000690
- Rockstrom, J., M. Falkenmark, T. Allan, C. Folke, L. Gordon, A. Jagerskog, M. Kumm, M. Lannerstad, M. Meybeck, D. Molden, S. Postel, H. H. G. Savenije, U. Svedin, A. Turton, and O. Varis 2014. The unfolding water drama in the Anthropocene: Towards a resilience-based perspective on water for global sustainability. *Ecohydrology* 7(5), 1249–1261, doi:10.1002/eco.1562.
- Sefton, C.E.M. and S.M. Howarth 1998. Relationships between dynamic response characteristics and physical descriptors of catchments in England and Wales. *J. Hydrology* 211(1-4), 1–16, doi:10.1016/s0022-1694(98)00163-2
- Seibert, J. 1999. Regionalisation of parameters for a conceptual rainfall-runoff model. *Agricul. Forest Meteorol.* 98-9, 279–293. doi:10.1016/s0168-1923(99)00105-7
- Seibert, J. and M. J. P. Vis 2012. Teaching hydrological modeling with a user-friendly catchment-runoff-model software package. *Hydrol. Earth System Sci.* 16(9), 3315–3325, doi:10.5194/hess-16-3315-2012
- Sigurðsson, F. 1990. Groundwater from glacial areas in Iceland. *Jökull* 40, 119–146.
- Sigurðsson, F. and K. Einarsson 1988 Groundwater resources of Iceland – Availability and demand. *Jökull* 38, 34–53.
- Sigurðsson, F., J.F. Jónsdóttir, S.G. Halldórsdóttir and T. Jóhannsson 2006. *Vatnafarsleg flokkun vatnasvæða Íslands*. OS-2006/013, 18 pp. National Energy Authority, Reykjavík.
- Steingrímsson, B., S. Björnsson and H. Adalsteinsson 2006. *Master plan for geothermal and hydropower development in Iceland*. Workshop for Decision Makers on Geothermal Projects in Central America, organized by UNU-GTP and LaGeo in San Salvador, El Salvador, 11 pp.
- Sun, W.C., H. Ishidaira and S. Bastola 2010. Towards improving river discharge estimation in ungauged basins: Calibration of rainfall-runoff models based on satellite observations of river flow width at basin outlet. *Hydrol. Earth System Sci.* 14(10), 2011–2022, doi:10.5194/hess-14-2011-2010
- Thirel, G., C. Notarnicola, M. Kalas, M. Zebisch, T. Schellenberger, A. Tetzlaff, M. Duguay, N. Molg, P. Burek and A. de Roo 2012. Assessing the quality of a real-time Snow Cover Area product for hydrological applications. *Remote Sensing Env.* 127, 271–287, doi:10.1016/j.rse.2012.09.006
- Þórarinsdóttir, T. 2012. Development of a methodology for estimation of Technical Hydropower potential in Iceland using high resolution Hydrological Modeling, 126 pp. Veðurstofa Íslands, Reykjavík.
- Tómasson, H. 1981. *Vatnsaft Íslands – Mat á stærð orkulindar*. National Energy Authority, Department of Hydropower, Reykjavík, 14pp.
- Wu, B., Y. Zheng, X. Wu, Y. Tian, F. Han, J. Liu and C. M. Zheng 2015. Optimizing water resources management in large river basins with integrated surface water-groundwater modeling: A surrogate-based approach. *Water Resources Res.* 51(4), 2153–2173, doi:10.1002/2014wr016653
- Xie, P.P. and P.A. Arkin 1997. Global precipitation: A 17-year monthly analysis based on gauge observations, satellite estimates, and numerical model outputs. *Bull. Am. Meteorol. Soc.* 78(11), 2539–2558, doi:10.1175/1520-0477(1997)078<2539:gpayma>2.0.co;2
- Xu, C.Y. and V.P. Singh 2004. Review on regional water resources assessment models under stationary and changing climate. *Water Res. Managem.* 18(6), 591–612, doi:10.1007/s11269-004-9130-0
- Xu, L., D. Marinova and X.M. Guo 2015. Resilience thinking: a renewed system approach for sustainability science. *Sustainability Science* 10(1), 123–138, doi:10.1007/s11625-014-0274-4
- Zhou, Y., M. Hejazi, S. Smith, J. Edmonds, H. Li, L. Clarke, K. Calvin and A. Thomson 2015. A comprehensive view of global potential for hydro-generated electricity. *Energy Environm. Sci.* 8(9), 2622–2633, doi:10.1039/c5ee00888c